A Proxy for Quantitative Sea Ice Reconstruction under Complicated Hydrodynamic Conditions: A Case Study in Prydz Bay, Antarctica

Jiaqi Wu[1], Zhengbing Han[1,*], Gaojing Fan[1], Jun Zhao[1], Haifeng Zhang[1], Jianming Pan[1,*], Sohey Nihashi[2], Baijuan Yang[1], Qiuhong Zhu[1], Haiyan Jin[1,3], Jianfang Chen[1,3]

[1] Key Laboratory of Marine Ecosystem Dynamics, Second Institute of Oceanography, Ministry of Natural Resources, Hangzhou, 310012, China.

[2] National Institute of Technology, Tomakomai College, Tomakomai 059-1275, Hokkaido, Japan.

[2] State Key Laboratory of Satellite Ocean Environment Dynamics, Second Institute of Oceanography, Ministry of Natural Resources, Hangzhou, 310012, China.

Corresponding author: Zhengbing Han (hzbing@sio.org.cn) and Jianming Pan (jmpan@sio.org.cn)

Key Points:

- We investigate the $IPSO_{25}$ and P_BIPSO_{25} (sea ice proxies) in a sediment trap and surface sediments from Prydz Bay, Antarctica.
- $IPSO_{25}$ and P_BIPSO_{25} in sediments would be affected by hydrodynamic conditions alongside its production mechanism.
- The accuracy of quantitative summer sea ice reconstruction increased from 22% based on P_BIPSO_{25} to 63% based on $P_BIPSO_{25\sigma}$.

Abstract

$IPSO_{25}$ and a combination of phytoplankton biomarkers and $IPSO_{25}$ (termed $PIPSO_{25}$) have been proposed as qualitative sea ice proxies in Antarctica. Exploring the effects of hydrodynamic conditions on the proxies might prompt the development of quantitative sea ice reconstruction. We investigated the variabilities of $IPSO_{25}$, brassicasterol, P_BIPSO_{25} (B indicates using brassicasterol as the phytoplankton biomarker) in a sediment trap, and the distributions of these proxies, and mean grain size and sorting (σ), which are indicators of hydrodynamic conditions in surface sediments from Prydz Bay. The proxy signals in sediments decoupled with the information from the upper layer reveal that the export of biomarkers to sediments would be affected by the hydrodynamic conditions. Accordingly, we normalized $IPSO_{25}$ and P_BIPSO_{25} to the sorting to compensate for different deposit environments. The accuracy of summer sea ice reconstruction increased from ca. 23% (based on $IPSO_{25}$ or P_BIPSO_{25} alone) to 63% (based on $P_BIPSO_{25} \times \sigma^2$).

Plain Language Summary

Antarctic sea ice plays a vital role in the global climate system. Understanding the variabilities of sea ice conditions in the long term could help in the accurate prediction of climate in the future. Recently, $IPSO_{25}$ and P_BIPSO_{25} have been proposed as alternative proxies for sea ice reconstruction alongside the traditional ice proxies based on microfossils in Antarctica. These proxies were based on the assumption that the chemical compound was produced by diatoms in the sea ice, subsequently sinking to and being preserved in the underlying seafloor. However, based on the results from a sediment trap and surface sediments from Prydz Bay, Antarctica, we found that the information of sea ice conditions reconstructed from $IPSO_{25}$ and P_BIPSO_{25} signals in sediments mismatched with satellite observations. This is attributed to the effect of current transport from the top to bottom sediments. Hence, we adjust the sea ice proxies to the grain size parameters which are indicators for current conditions to offset the effects of the currents. The accuracy of sea ice reconstruction increased from ca. 23% based on $IPSO_{25}$ or P_BIPSO_{25} alone to 63% based on $P_BIPSO_{25\sigma}$ which is the P_BIPSO_{25} proxy normalized to grain size parameters.

1 Introduction

The complex figure (satellite observations) of Antarctic sea ice shows that sea ice modestly increased to an overall extent (with opposing regional trends) during 1979–2014 (Maksym, 2019), followed by an unprecedented and consistent decline in all regions (Parkinson, 2019). Sea ice play a vital role in the climate system by affecting the ecosystem (Arrigo, 2014) and global carbon cycle (Stephens & Keeling, 2000), regulating the exchange of heat and gas between the atmosphere and ocean (Thomas, 2017), and driving the formation of bottom water (Ohshima et al., 2013), so it is essential to understand that the mechanisms controlling the variabilities. One of the methods is to determine the changes in sea ice before direct observations through sea ice proxies (de Vernal et al., 2013).

Studies of paleo sea ice reconstruction in polar regions are commonly based on microfossils (foraminiferal assemblages and diatoms) associated with sea ice. However, their application may be limited by the selective degradation of the microfossils in the water column and sediments (de Vernal et al., 2013). Recently, a suite of highly branched isoprenoids (HBIs) has been proposed as alternative or additional sea ice proxies in the Arctic and Antarctica (Belt, 2018). A mono-unsaturated C_{25} HBI called IP_{25} is considered a sea ice biomarker in the Arctic

(Belt et al., 2007). The source of IP_{25}, its time-series studies, and modern spatial distributions (over 500 samples) have been investigated to evaluate its applicability for the qualitative reconstruction of sea ice (Belt et al., 2008; Brown et al., 2011, 2014). Other biomarkers (brassicasterol) have been combined with IP_{25} (the so-called PIP_{25} index) to improve the quality of sea ice reconstructions (Müller et al., 2009, 2011; Stein et al., 2016). Further, IP_{25} and PIP_{25} proxies have been calibrated with sea ice concentrations (SIC) to explore their potential for quantitative sea ice reconstruction (Belt, 2018). Interestingly, IP_{25} has not been found in Antarctica. A di-unsaturated C_{25} HBI (termed as $IPSO_{25}$; Fig. S1), a structure analog of IP_{25}, has been confirmed as a product of sea ice algae by the identification of the algal products, $\delta^{13}C$ value of $IPSO_{25}$ in sediments, and its distribution characteristics in the surface water column and surface sediments (Belt et al., 2016; Smik et al., 2016; Vorrath et al., 2019). Hence, $IPSO_{25}$ and the combined index of phytoplankton biomarkers and $IPSO_{25}$ (termed $PIPSO_{25}$) following the PIP_{25} index in the Arctic have been considered as promising sea ice proxies in Antarctica (Massé et al. 2011; Vorrath et al. 2019). Further, the highest concentrations of $IPSO_{25}$ are located in coastal areas, which are partially covered by land-fast ice (fast ice), together with the only known producer of $IPSO_{25}$, *Berkeleya adeliensis* (Medlin) which is the dominant species on fast ice, leading to the proposal that $IPSO_{25}$ signals might reflect the ice types (Belt et al., 2016). However, variations in $IPSO_{25}$ distributions might be caused by factors apart from sea ice conditions such as hydrodynamic conditions. It has been reported that biomarker records (e.g., n-alkanes, lignin, GDGTs, IP_{25}) could be affected by hydrodynamic sorting as they reside in different particle size fractions (Feng et al., 2013; Mollenhauer et al., 2006; Navarro-Rodriguez et al., 2013). Therefore, we hypothesize that the accuracy of sea ice reconstruction based on $IPSO_{25}$ and $PIPSO_{25}$ might be affected by hydrodynamic conditions.

As such, we investigated the temporal variations in $IPSO_{25}$ and phytoplankton biomarkers (and calculated $PIPSO_{25}$) from a sediment trap deployed at Prydz Bay (PB), and compared these with the SIC to explore the effects of the deposition process on the distribution of these proxies in sediments. We established the distribution of these proxies in surface sediments from PB, and compared $IPSO_{25}$ and $PIPSO_{25}$ with the satellite-derived sea ice types. We analyzed the grain size parameters which are indicators for hydrodynamic conditions. These parameters, along with SIC, were combined with sea ice proxies to further explore the potential of these indices for the quantitative reconstruction of paleo-sea ice.

2 Materials and methods

2.1 Study area

PB (Fig.1) is the largest continental embayment in East Antarctica. The oceanic circulation in PB is composed of a closed cyclonic gyre called the Prydz Bay Gyre (PBG) and a narrow westward Antarctic Coastal Current (ACC) along the face of the Amery Ice Shelf (AIS) (Williams et al., 2016). In PB, sea ice freezes from March until reaching its maximum value in September. The sea ice then begins to melt in October, reaching its minimum value in February of the following year (Zheng, 2011). The types of sea ice in PB comprise fast ice, pack ice, and polynyas. Fast ice is restricted to the vicinity of the AIS (Nihashi & Ohshima, 2015). There are two polynyas named the Mackenzie polynya (MP) and Barrier polynya (BP). The rest of the study area is covered by pack ice in the austral winter. There were nine types of sediments in the PB. Silt and slightly gravelly sediments were mainly located in central PB and the Four Ladies

Bank (FLB), while sandy silt and slightly gravelly muddy sand were widely distributed in the Fram Bank (FB) and the front of the AIS (Wang et al., 2015).

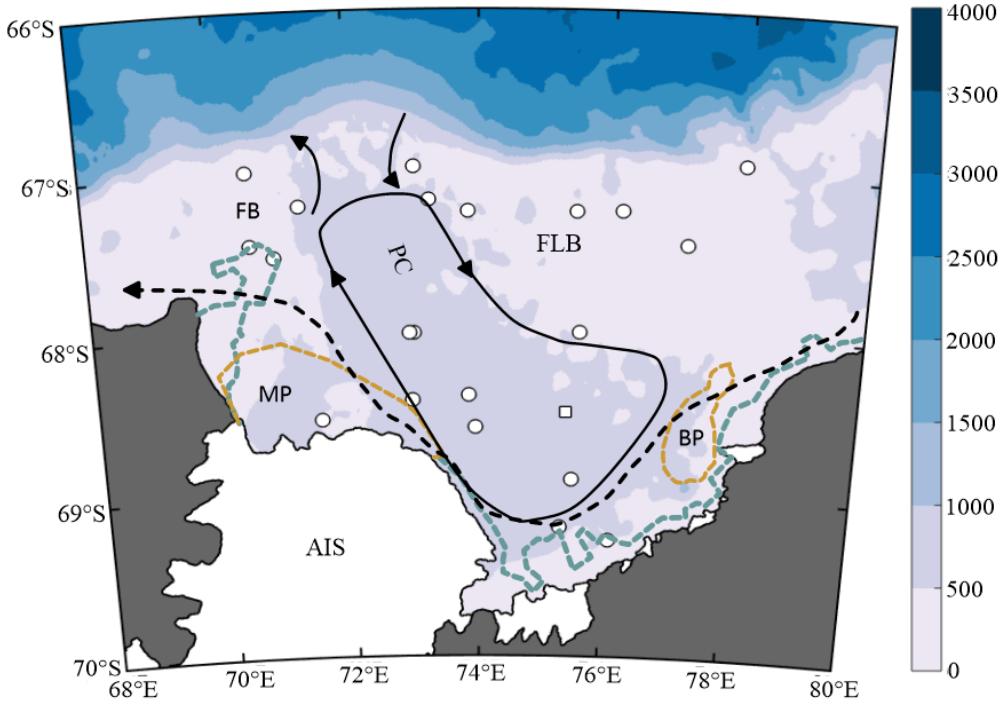

Figure 1. Map of PB showing the sampling locations and oceanographic setting. The locations of the sediment trap and surface sediments are shown as a black square and white dots, respectively. The black lines are the PBG and the black dashed line is the ACC. The yellow dashed line indicates the location of the MP and BP. The green dashed line delineates the boundary of the landfast ice with the frequency of its occurrence higher than 60% during the period 2003–2011 (Nihashi & Ohshima, 2015). The contour shows the bathymetry (Fretwell et al. 2013).

2.2 Sediment sampling

The sediment trap (McLane, USA) was deployed at PB (M7, 75.38° E, 68.49° S; water depth: 620 m; Fig.1, Table S1) during the 30th Chinese National Antarctic Research Expedition (CHINARE) and installed 490 m below the sea surface. After recovery, three of the aliquots collected during October, 2014 to February, 2015 were used for the particulate organic carbon (POC), biogenic silica (BSi), and biomarker analyses. Further details are described in Han et al. (2018) and the supporting information.

Surface sediment samples were collected during the CHINARE cruises in 2009, 2011, and 2013 using a box corer (Fig.1, Table S2). All samples after collection were preserved at -20 °C until the analyses of total organic carbon content (TOC), grain size, and biomarkers were conducted.

2.3 POC, BSi, TOC, grain size, and biomarker analyses

The analyses of POC and TOC followed Han et al. (2019) and (Sun et al. 2016). Briefly, after removing the inorganic carbon (Schumacher, 2002), the carbon content of each sample was measured using an elemental analyzer (Elementar, Germany). A sodium carbonate leaching analysis procedure was used to determined BSi concentration as described in Han et al. (2019).

The unground samples were scattered by a $Na_4P_2O_7$ solution prior to the analysis. The grain size was analyzed using a laser particle size analyzer (Malvern 3000). The grain-size parameters, including the mean grain size (Mz) and sorting (σ) were calculated graphically following Folk (1968).

For biomarker analyses, in brief, the internal standards, including 7-hexylnonadecane (provided by Simon Belt from Plymouth University) and cholest-5-en-3β-ol-D6, were added to the freeze-dried samples before the extraction. Samples were extracted in ultrasonication. HBIs and sterols were purified using the silica gel chromatography. Furthermore, sterols were derivatized with BSTFA. Both fractions were analyzed using an Agilent gas chromatography coupled to a mass selective detector. Further details concerning biomarker analyses are described in Belt et al. (2012), Smik (2016) and supporting information (Text S1).

2.4 Calculation of $PIPSO_{25}$

The $PIPSO_{25}$ indices were calculated according to the equation (Vorrath et al., 2019):

$$PIPSO_{25} = \frac{IPSO_{25}}{IPSO_{25} + phytoplankton \times c} \quad (1)$$

The detailed calculation of the balance factor *c* is described in supporting information (Text S2). Diatom biomarkers were chosen to represent the phytoplankton biomarker as phytoplankton is mainly composed of diatoms (> 80%) that are the main component of the settling particles in summer in PB (Han et al., 2019; Sun et al., 2003). Brassicasterol and HBI III (a tri-unsaturated C_{25} HBI; Fig. S1) have been recognized as phytoplankton diatom biomarkers (Massé et al., 2011; Müller et al., 2009; Rampen et al., 2010). Brassicasterol was used to calculate P_BIPSO_{25}, and HBI III was used to calculate $P_{III}IPSO_{25}$.

2.5 Data presentation and storage

The daily SIC data used in this study were obtained from the Institute of Environmental Physics at the University of Bremen (Spreen et al., 2008). The remote sensing chlorophyll a (Chl a) data derived from the European Space Agency (ESA). The detailed calculation of SIC and Chl a used in this study were described in supporting information (Text S3).

3 Results

3.1 Temporal variability in environmental conditions and the fluxes and/or concentrations of POC, BSi, and biomarkers

According to satellite observations, the sea ice melting season at the M7 started on November 18, 2014 and ended on November 26, 2014. The site was then ice-free until refrozen in March. Furthermore, ice floes were observed twice at the end of November and December, respectively (Fig. 2a). After large-scale sea ice melting, the surface Chl a concentration increased gradually and reached a maximum in mid-January 2015 (Fig. 2a).

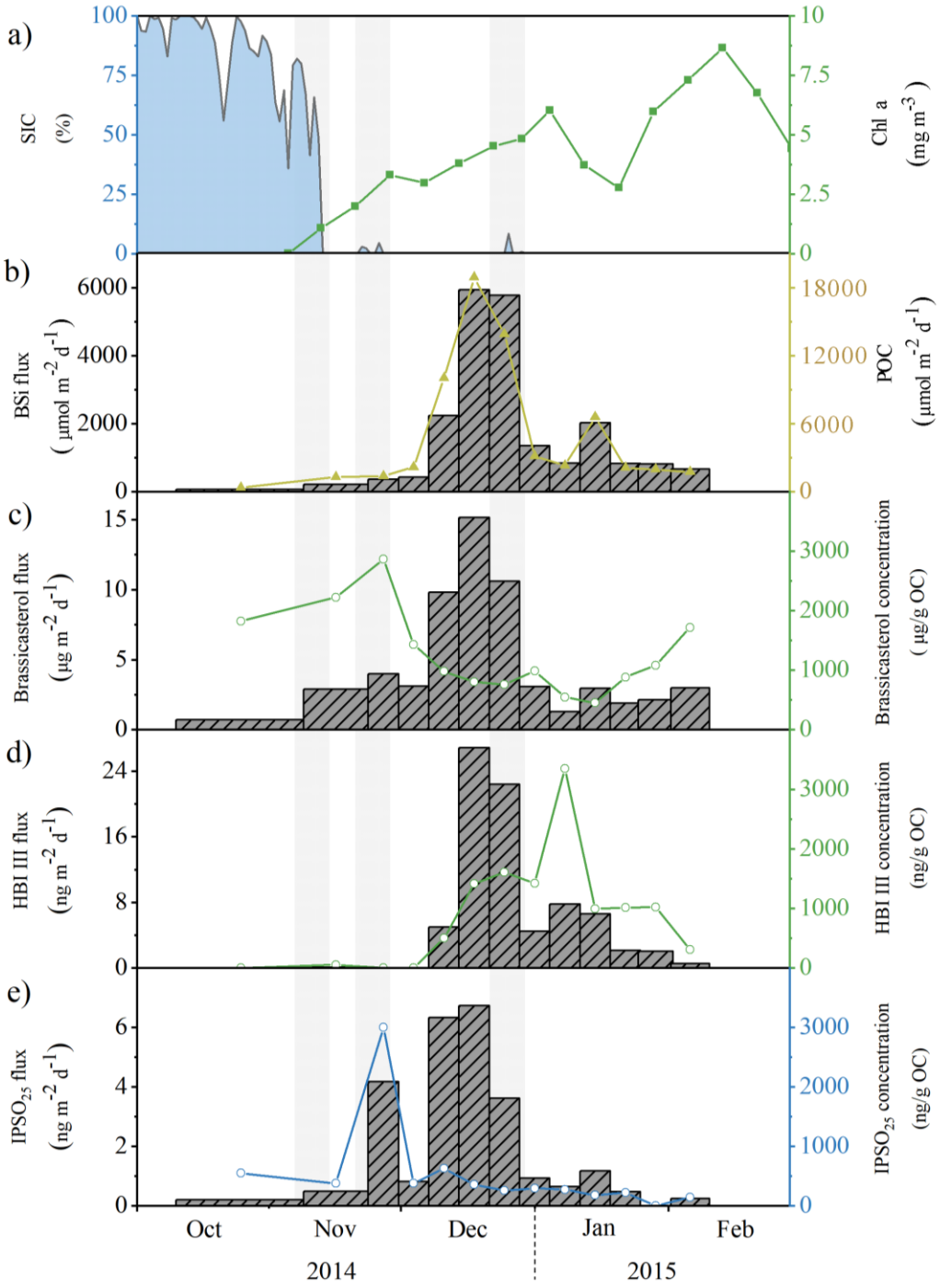

Figure 2. Time series of the bulk parameters, biomarkers, and P_BIPSO_{25} values measured at station M7 from October, 2014 to February, 2015. (a) Satellite-derived SIC (Spreen et al. 2008) and Chl a (https://www.esa.int/); (b) BSi and POC flux; fluxes and concentrations of brassicasterol (c), HBI III (d), and $IPSO_{25}$ (e). The grey shades indicate the events of sea ice melting.

During the study period, the average fluxes of POC and BSi were 508.99 μmol m^{-2} d^{-1} and 2034.63 μmol m^{-2} d^{-1}, respectively (Fig. 2b). Brassicasterol was detected in all samples (Fig. 2c). Brassicasterol flux increased after the sea ice melted and peaked abruptly in mid-December. Its concentration ranged from 448.40 to 2868.46 μg/g OC; the temporal variation trend of brassicasterol concentration was similar to that of Chl a. HBI III was present in most samples, apart from those collected during late spring (Fig. 2d). The HBI III flux abruptly peaked at 26.85 ng m^{-2} d^{-1}, subsequently decreasing until the end of the sample collection period. Its concentration increased to its highest (3353.69 ng/g OC) in early January 2015 and subsequently decreased drastically. The trend pattern of HBI III concentration is different from that of brassicasterol, which might be caused by HBI III degradation as it is more vulnerable to degradation than brassicasterol (Rontani et al., 2011, 2019). Hence, we do not evaluate the applicability of $P_{III}IPSO_{25}$ in this paper.

$IPSO_{25}$ was detected in all the trap samples except for that collected from January 26, 2015 to February 3, 2015 (Fig. 2e). The highest concentration of $IPSO_{25}$ occurred in the end of November (3003.56 ng/g OC). $IPSO_{25}$ flux peaked in the end of November (4.17 ng m^{-2} d^{-1}) and mid-December (6.73 ng m^{-2} d^{-1}) and then decreased drastically after the occurrence of the second peak.

3.2 Spatial distributions of TOC, grain size, and biomarkers

The TOC values ranged from 0.2 to 1.87% (Table 1). The average values of TOC were similar in the fast ice (1.04 ± 0.84 %) and non-fast ice zones (including the pack ice and polynya zones; 0.90 ± 0.40 %). The value of sorting ranges from 1.45 to 2.76 φ, and shows a disparity between the fast ice and non-fast ice zones. For the fast ice zone, the average sorting value is 1.88 ± 0.41 φ, indicating a poorly sorted condition; for the non-fast ice zone, the average sorting value is 2.14 ± 0.43 φ, indicating a very poorly sorted condition (Table 1; Fig. S4).

The concentration of brassicasterol ranged from 62.04 to 290.47 μg/g OC (Table 1; Fig. S3). The average brassicasterol concentration in the fast ice zone (87.87 ± 32.21 μg/g OC) was lower than that in the non-fast ice zone (98.70 ± 96.63 μg/g OC). Increased concentrations of brassicasterol were found in the region close to the continental slope between 67° S and 68° S, which is in accordance with the satellite-derived Chl a maximum (Herraiz-Borreguero et al., 2016, Fig. 2a), and align well with the BSi distribution pattern in Prydz Bay from (Harris et al., 1998; Hu et al., 2007). This additionally supports the use of brassicasterol as a diatom proxy in the study area. The distribution pattern of HBI III is in contrast to that of brassicasterol: the average concentration of HBI III in the fast ice zone is twice that in the non-fast ice zone (Table 1; Fig. S4).

$IPSO_{25}$ was detected in all surface sediment samples, with average values up to 791.13 ± 384.58 ng/g OC in the fast ice zone to 179.49 ± 200.02 ng/g OC in the non-fast ice zone (Table 1; Fig. S3). The distribution pattern of P_BIPSO_{25} was similar to that of $IPSO_{25}$ (Table 1; Fig. S4), with the average value of P_BIPSO_{25} in the fast ice zone (0.74 ± 0.07) being twice that in the non-fast ice zone (0.34 ± 0.18).

4 Discussion

4.1 Seasonal variability of biomarkers and its linkage with sea ice conditions

Diatoms are the main constituent of phytoplankton in PB. The mismatch between the BSi fluxes and the changes in the phytoplankton biomass represented by satellite Chl a data might be affected by the dissolution and/or lateral transport of BSi in the deposition process (Fig. 2a, b). However, there was a significant correlation between the fluxes of BSi and brassicasterol, which is resistant to degradation (R^2=0.81, p<0.01), indicating that the mismatch between the fluxes of phytoplankton proxies and phytoplankton biomass might mainly be caused by the lateral transport. Lateral transport is mainly controlled by sinking rates; ballast materials (i.e., opal, $CaCO_3$, and lithogenic minerals) attached to sinking particles could affect the deposition velocities (Alldredge & Gotschalk, 1988). However, it has been suggested that opal is not an efficient ballast material during diatom blooms as they tend to form low-density aggregates in the water column (Bach et al., 2016). Therefore, at the beginning of the ice-free period, lithogenic materials derived from the melting ice floe attached to the phytoplankton aggregates, thereby increasing the velocities of the aggregates, which in-turn increased the BSi and brassicasterol fluxes. In contrast, the sinking rates decreased when there was no melting of ice, and hence decreased the amount of lithogenic materials. Therefore, the residence time of phytoplankton in the water column was extended and phytoplankton aggregates were more susceptible to being carried by the current, leading to low fluxes of BSi and brassicasterol when the phytoplankton biomass increased.

The patterns of $IPSO_{25}$ fluxes, to some extent, link with the sea ice conditions. During the strict ice-free period (without ice floe melting events), the $IPSO_{25}$ flux and concentrations were extremely low or undetectable, consistent with the finding that the flux of the ice algae proxy was low during this period in the Arctic from Bai et al. (2019) and Fahl and Stein (2012). During the melting season (late spring and summer), the biomass of sea ice algae sharply increases when the strength of the light increases in polar regions. Moreover, the ice algae are subsequently deposited to the underlying sediments when the ice melts (McMinn et al., 2010). Thus, $IPSO_{25}$ fluxes should evidently increase during the melting season (Bai et al., 2019). However, in this study, the $IPSO_{25}$ fluxes did not increase during large-scale sea ice melting in mid-November. This might be due to the ex-situ melting of sea ice and/or the ice algae from the melting ice being carried elsewhere by strong currents. Additionally, there were time lags between the peak of $IPSO_{25}$ fluxes and ice floe melting events, likely due to hydrodynamic conditions. As such, although $IPSO_{25}$ could be used for qualitative sea ice reconstruction to some extent, the effects of hydrodynamics cannot be ignored when the proxy is used for quantitative sea ice reconstruction.

4.2 Testing the applicability of the combined open-water phytoplankton biomarkers and $IPSO_{25}$ in different sea ice conditions

The spatial distribution pattern of $IPSO_{25}$ likely refers to the different sea ice types, with the highest $IPSO_{25}$ concentrations located in the fast ice zone and lower $IPSO_{25}$ concentrations in the non-fast ice zone, which is consistent with the results of Belt et al. (2016). Owing to the different processes of sea ice formation, the ice structures in the fast ice and non-fast ice zones are different (Allison, 1989). Columnar ice is the main component in the fast ice zone; as for the non-fast ice zone, the ice contains significant amounts of frazil ice (Gow et al., 1982; He et al., 1998), leading to different ice algae compositions in the two regions (Ackley & Sullivan, 1994;

Scott et al., 1994). For example, *B. adeliensis* is recognized as one of the dominant species in the bottom section of fast ice, but not in pack ice (Riaux-Gobin et al., 2003; Saggiomo et al., 2017). This might lead to a disparity in the distribution patterns of $IPSO_{25}$ in the two regions. Additionally, the phytoplankton biomass (brassicasterol concentrations) in the fast ice zone was slightly lower than that in the non-fast ice zone, and when combined with the characteristics of the $IPSO_{25}$ distribution pattern, it leads to higher P_BIPSO_{25} values in the fast ice zone.

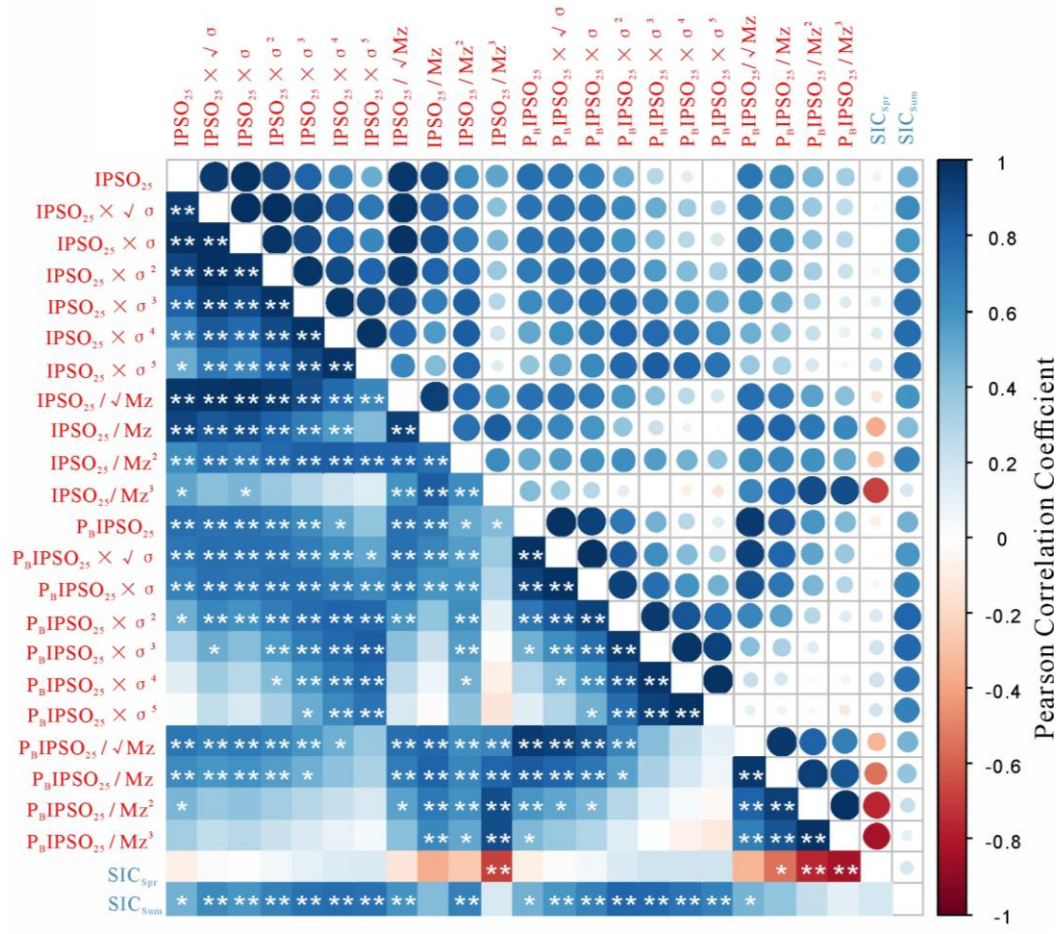

Figure 3. Pearson correlation coefficients of sea ice proxies with the mean austral spring SIC and austral summer SIC. The dot size and the color indicate the magnitude of the correlation coefficients. Single asterisk and double asterisks indicate that the correlation is significant at a level of 0.05 (2-tailed) and of 0.01 (2-tailed), respectively.

To further test the applicability of $IPSO_{25}$ and P_BIPSO_{25} for quantitative sea ice reconstruction, we compared the $IPSO_{25}$ concentrations and P_BIPSO_{25} values with spring SIC (SIC_{Spr}) and summer SIC (SIC_{Sum}). Both $IPSO_{25}$ concentrations and P_BIPSO_{25} values did not exhibit any clear correlation with SIC_{Spr} but showed a positive correlation with SIC_{Sum} (Fig. 3), suggesting that the proxies are mainly affected by the presence of summer sea ice. Indeed, the sympagic algae biomass sharply increases during the ice melting season, and sea ice melts

quickly during summer in PB (Günther & Dieckmann, 1999; Lei et al., 2010; Zheng, 2011). Further, the linear correlation of $IPSO_{25}$ and P_BIPSO_{25} against SIC_{Sum} can be described as:

$$IPSO_{25} = 10.123 \times SIC_{Sum} - 16.786 \ (R^2 = 0.23, p < 0.05) \quad (2)$$

$$P_BIPSO_{25} = 0.0067 \times SIC_{Sum} + 0.2082 \ (R^2 = 0.22, p < 0.05) \quad (3)$$

However, the accuracy of the sea ice reconstruction based on $IPSO_{25}$ or P_BIPSO_{25} alone is only ~ 23%, which might be attributed to $IPSO_{25}$ concentrations in sediments being affected by the hydrodynamic conditions during the sinking processes as mentioned before, alongside the sea ice conditions. Hydrodynamic conditions may trigger the lateral transport and differentiation of biomarker records residing within the different particle classes, and then the decoupling of proxies (Kim et al., 2009; Mollenhauer et al., 2006). Grain size parameters such as the Mz and sorting have been used as indicators of hydrodynamic energy for particles undergoing sediment processes (Robert Louis Folk & Ward, 1957; Prodger et al., 2016). The Mz in the fast ice zone is larger than that in the non-fast ice zone, and the sorting value in the fast ice zone is lower than that in the non-fast ice zone (Table 1), indicating a stronger hydrodynamic condition of sedimentation in the fast ice zone. In a stronger sorting environment (fast ice zone), the deposition of fine particles is difficult as their sinking rate is slower than the current speed (McCave & Hall, 2006; Yoon et al., 1998). Large parts of organic carbon are associated with smaller particles because of their high surface area (Mayer, 1994), likely leading to the loss of organic carbon, which is absorbed in a fine fraction. However, ice algae are subject to relatively rapid sedimentation as they tend to form aggregates and the lithogenic material derived from melting ice can be incorporated into the aggregates, enhancing their sinking velocities (Han et al., 2019; Riebesell et al., 1991; Van der Jagt et al., 2018). Thus, in the fast ice zone, the material derived from the ice algae contributes greatly to the organic carbon than that derived from the ice algae in the non-fast ice zone. In contrast, in a weaker sorting environment (non-fast ice zone), the deposition of small sized particles is relatively easy; this, along with a higher biomass of phytoplankton, leads to the dilution of the $IPSO_{25}$ signals. Overall, the $IPSO_{25}$ concentrations and P_BIPSO_{25} values in the fast ice zone were higher than those in the non-fast ice zone. Accordingly, we normalized the $IPSO_{25}$ concentrations and P_BIPSO_{25} by introducing the Mz and sorting (σ) to compensate for the different hydrodynamic conditions and calculated the possible combinations. Most of the normalized sea ice proxies show better correlations with SIC_{Sum} (Fig. 3), suggesting that this approach provides a more reliable approach for sea ice reconstruction. The highest correlations between normalized proxies and SIC_{Sum} are as follows:

$$P_BIPSO_{25\sigma} = P_BIPSO_{25} \times \sigma^2 \quad (4)$$

$$P_BIPSO_{25\sigma} = 0.0458 \times SIC_{Sum} + 0.3 \ (R^2 = 0.63, p < 0.01) \quad (5)$$

The accuracy of the summer sea ice reconstruction significantly increased from 22% based on the sea ice proxies without normalization to 64% based on the normalized sea ice proxy (i.e., $P_BIPSO_{25\sigma}$). This indicates that the introduction of sorting to sea ice proxies can effectively boost their certainty for summer sea ice reconstructions in the study area. However, further work is necessary to evaluate the applicability of this approach in other Antarctic regions.

5 Conclusions

The mismatch between the records of $IPSO_{25}$ and P_BIPSO_{25} in sediments and the information from the upper layer was attributed to the effect of the deposition process on their

distribution. Therefore, the use of these proxies alone to reconstruct sea ice conditions should be cautious. The normalization of $IPSO_{25}$ and P_BIPSO_{25} to sorting increases the precision of these proxies for summer sea ice reconstruction in complex sedimentary environments. The accuracy of summer sea ice reconstruction increased from 22% based on $IPSO_{25}$ or P_BIPSO_{25} alone to 63% based on $P_BIPSO_{25\sigma}$, providing a promising method for the quantitative summer sea ice reconstruction in Antarctica.

Acknowledgments, Samples, and Data

We thank the captains, crew, and science party of the RV "Xuelong" for their assistance in the sample collection. Additionally, we thank Simon Belt (University of Plymouth) for providing the inter standard (7-hexylnonadecane). Datasets for this research are included in this paper (and its supplementary information files). The original fast ice data can be found from https://kosenjp-my.sharepoint.com/:f:/g/personal/sohey_tomakomai_kosen-ac_jp/Eojgxb19Pn1Jv4Dof6bVb_MBzS1cgT1btVrNXBDdTURhIw?e=KUcJYs (and Dataset s1). The original SIC data can be found from the Institute of Environmental Physics at the University of Bremen (https://seaice.uni-bremen.de/databrowser/). The original Chl a data can be found from the ESA (https://www.esa.int/). This research was supported by the National Natural Science Foundation of China (41976227, 41976228, and 41376193) and the response and feedback of the Southern Ocean to climate change (RFSOCC2020-2025). Authors declare no competing interests.

References

Ackley, S. F., & Sullivan, C. W. (1994). Physical controls on the development and characteristics of Antarctic sea ice biological communities—a review and synthesis. *Deep Sea Research Part I: Oceanographic Research Papers*, *41*(10), 1583–1604. https://doi.org/10.1016/0967-0637(94)90062-0

Alldredge, A. L., & Gotschalk, C. (1988). In situ settling behavior of marine snow 1. *Limnology and Oceanography*, *33*(3), 339–351. https://doi.org/10.4319/lo.1988.33.3.0339

Allison, I. (1989). The East Antarctic Sea Ice Zone: Ice Characteristics and Drift. *GeoJournal*, *18*(1), 103–115. https://doi.org/10.1007/BF00722394

Arrigo, K. R. (2014). Sea ice ecosystems. *Annual Review of Marine Science*, *6*, 439–467. https://doi.org/10.1146/annurev-marine-010213-135103

Bach, L. T., Boxhammer, T., Larsen, A., Hildebrandt, N., Schulz, K. G., & Riebesell, U. (2016). Influence of plankton community structure on the sinking velocity of marine aggregates. *Global Biogeochemical Cycles*, *30*(8), 1145–1165. https://doi.org/10.1002/2016GB005372

Bai, Y., Sicre, M.-A., Chen, J., Klein, V., Jin, H., Ren, J., Li, H., Xue, B., Ji, Z., Zhuang, Y., & Zhao, M. (2019). Seasonal and spatial variability of sea ice and phytoplankton biomarker flux in the Chukchi sea (western Arctic Ocean). *Progress in Oceanography*, *171*, 22–37. https://doi.org/10.1016/j.pocean.2018.12.002

Belt, S. T. (2018). Source-specific biomarkers as proxies for Arctic and Antarctic sea ice. *Organic Geochemistry*, *125*, 277–298. https://doi.org/10.1016/j.orggeochem.2018.10.002

Belt, S. T., Brown, T. A., Rodriguez, A. N., Sanz, P. C., Tonkin, A., & Ingle, R. (2012). A reproducible method for the extraction, identification and quantification of the Arctic sea

ice proxy IP25 from marine sediments. *Anal.Methods*, *4*, 705–713. https://doi.org/10.1039/c2ay05728j

Belt, S. T., Massé, G., Rowland, S. J., Poulin, M., Michel, C., & LeBlanc, B. (2007). A novel chemical fossil of palaeo sea ice: IP25. *Organic Geochemistry*, *38*(1), 16–27. https://doi.org/10.1016/j.orggeochem.2006.09.013

Belt, S. T., Massé, G., Vare, L. L., Rowland, S. J., Poulin, M., Sicre, M.-A., Sampei, M., & Fortier, L. (2008). Distinctive 13C isotopic signature distinguishes a novel sea ice biomarker in Arctic sediments and sediment traps. *Marine Chemistry*, *112*(3), 158–167. https://doi.org/10.1016/j.marchem.2008.09.002

Belt, S. T., Smik, L., Brown, T. A., Kim, J.-H., Rowland, S. J., Allen, C. S., Gal, J.-K., Shin, K.-H., Lee, J. I., & Taylor, K. W. R. (2016). Source identification and distribution reveals the potential of the geochemical Antarctic sea ice proxy IPSO25. *Nature Communications*, *7*, 12655. https://doi.org/10.1038/ncomms12655

Brown, T. (2011). *Production and preservation of the Arctic sea ice diatom biomarker IP25*, (Doctoral dissertation). Retrieved from PEARL. (http://hdl.handle.net/10026.1/314). Plymouth: University of Plymouth.

Brown, T. A., Belt, S. T., Philippe, B., Mundy, C. J., Massé, G., Poulin, M., & Gosselin, M. (2011). Temporal and vertical variations of lipid biomarkers during a bottom ice diatom bloom in the Canadian Beaufort Sea: further evidence for the use of the IP25 biomarker as a proxy for spring Arctic sea ice. *Polar Biology*, *34*(12), 1857–1868. https://doi.org/10.1007/s00300-010-0942-5

Brown, T. A., Belt, S. T., Tatarek, A., & Mundy, C. J. (2014). Source identification of the Arctic sea ice proxy IP25. *Nature Communications*, *5*, 4197. https://doi.org/10.1038/ncomms5197

de Vernal, A., Gersonde, R., Goosse, H., Seidenkrantz, M.-S., & Wolff, E. W. (2013). Sea ice in the paleoclimate system: the challenge of reconstructing sea ice from proxies--an introduction. *Quaternary Science Reviews*, *79*, 1–8. https://www.sciencedirect.com/science/article/pii/S0277379113003089

Fahl, K., & Stein, R. (2012). Modern seasonal variability and deglacial/Holocene change of central Arctic Ocean sea-ice cover: New insights from biomarker proxy records. *Earth and Planetary Science Letters*, *351-352*, 123–133. https://doi.org/10.1016/j.epsl.2012.07.009

Feng, X., Vonk, J. E., van Dongen, B. E., Gustafsson, Ö., Semiletov, I. P., Dudarev, O. V., Wang, Z., Montluçon, D. B., Wacker, L., & Eglinton, T. I. (2013). Differential mobilization of terrestrial carbon pools in Eurasian Arctic river basins. *Proceedings of the National Academy of Sciences of the United States of America*, *110*(35), 14168–14173. https://doi.org/10.1073/pnas.1307031110

Folk, R. L. (1968). Petrology of sedimentary rocks. Austin, Texas: Hemphill's.

Folk, R. L., & Ward, W. C. (1957). Brazos River bar; a study in the significance of grain size parameters. *Journal of Sedimentary Research*, *27*(1), 3–26. https://doi.org/10.1306/74D70646-2B21-11D7-8648000102C1865D

Fretwell, P., Pritchard, H. D., Vaughan, D. G., Bamber, J. L., Barrand, N. E., Bell, R., Bianchi, C., Bingham, R. G., Blankenship, D. D., Casassa, G., Catania, G., Callens, D., Conway, H.,

399 Cook, A. J., Corr, H. F. J., Damaske, D., Damm, V., Ferraccioli, F., Forsberg, R., …
400 Zirizzotti, A. (2013). Bedmap2: improved ice bed, surface and thickness datasets for
401 Antarctica. *The Cryosphere*, *7*, 375–393. https://doi.org/10.5194/tc-7-375-2013

402 Gow, A. J., Ackley, S. F., Weeks, W. F., & Govoni, J. W. (1982). Physical and Structural
403 Characteristics of Antarctic Sea Ice. *Annals of Glaciology*, *3*, 113–117.
404 https://doi.org/10.3189/S0260305500002627

405 Günther, S., & Dieckmann, G. S. (1999). Seasonal development of algal biomass in snow-
406 covered fast ice and the underlying platelet layer in the Weddell Sea, Antarctica. *Antarctic*
407 *Science / Blackwell Scientific Publications*, *11*(3), 305–315.
408 https://doi.org/10.1017/S0954102099000395

409 Han, Z., Hu, C., Sun, W., Zhao, J., Pan, J., Fan, G., & Zhang, H. (2019). Characteristics of
410 particle fluxes in the Prydz Bay polynya, Eastern Antarctica (in Chinese with English
411 abstract). *SCIENCE CHINA Earth Sciences*, *62*(4), 657–670.
412 https://doi.org/10.1007/s11430-018-9285-6

413 Han, Z., Sun, W., Fan, G., Hu, C., Pan, J., Zhao, J., Zhang, H., Li, D., & Zhang, H. (2018).
414 Sinking particle fluxes during austral summer in the Prydz Bay polynya, Antarctica. *China*
415 *Environmental Science*, *38*(5), 1923–1934.

416 Harris, P. T., Taylor, F., Pushina, Z., Leitchenkov, G., O'Brien, P. E., & Smirnov, V. (1998).
417 Lithofacies distribution in relation to the geomorphic provinces of Prydz Bay, East
418 Antarctica. *Antarctic Science / Blackwell Scientific Publications*, *10*(3), 227–235.
419 https://doi.org/10.1017/S0954102098000327

420 He, J., Chen, B., & Wu, K. (1998). Developing and Structural Characteristics of First-Year Sea
421 Ice and With Effects on Ice Alage Biomass of Zhongshan Station,East Antarctica. *Journal*
422 *of Glaciology and Geocryology*, *20*(4), 358–367.

423 Herraiz-Borreguero, L., Lannuzel, D., van der Merwe, P., Treverrow, A., & Pedro, J. B. (2016).
424 Large flux of iron from the Amery Ice Shelf marine ice to Prydz Bay, East Antarctica:
425 MARINE ICE IRON FERTILIZES PRYDZ BAY. *Journal of Geophysical Research, C:*
426 *Oceans*, *121*(8), 6009–6020. https://doi.org/10.1002/2016JC011687

427 Hu, C., Yao, M., Yu, P., Pan, J., & Zhang, H. (2007). Biogenic silica in surficial sediments of
428 Prydz Bay of the Southern Ocean (in Chinese with English abstract). *Acta Oceanologica*
429 *Sinica*, *29*(5), 48–54. https://doi.org/10.3724/SP.J.1084.2013.00105

430 Kim, J.-H., Crosta, X., Michel, E., Schouten, S., Duprat, J., & Sinninghe Damsté, J. S. (2009).
431 Impact of lateral transport on organic proxies in the Southern Ocean. *Quaternary Research*,
432 *71*(2), 246–250. https://doi.org/10.1016/j.yqres.2008.10.005

433 Lei, R., Li, Z., Cheng, B., Zhang, Z., & Heil, P. (2010). Annual cycle of landfast sea ice in Prydz
434 Bay, east Antarctica. *Journal of Geophysical Research*, *115*(C2), 161.
435 https://doi.org/10.1029/2008JC005223

436 Massé, G., Belt, S. T., Crosta, X., Schmidt, S., Snape, I., Thomas, D. N., & Rowland, S. J.
437 (2011). Highly branched isoprenoids as proxies for variable sea ice conditions in the
438 Southern Ocean. *Antarctic Science / Blackwell Scientific Publications*, *23*(5), 487–498.
439 https://doi.org/10.1017/S0954102011000381

Mayer, L. M. (1994). Surface area control of organic carbon accumulation in continental shelf sediments. *Geochimica et Cosmochimica Acta*, *58*(4), 1271–1284. https://doi.org/10.1016/0016-7037(94)90381-6

McCave, I. N., & Hall, I. R. (2006). Size sorting in marine muds: Processes, pitfalls, and prospects for paleoflow-speed proxies. *Geochemistry, Geophysics, Geosystems*, *7*(10), Q10N05. https://doi.org/10.1029/2006GC001284

McMinn, A., Martin, A., & Ryan, K. (2010). Phytoplankton and sea ice algal biomass and physiology during the transition between winter and spring (McMurdo Sound, Antarctica). *Polar Biology*, *33*(11), 1547–1556. https://doi.org/10.1007/s00300-010-0844-6

Meehl, G. A., Arblaster, J. M., Chung, C. T. Y., Holland, M. M., DuVivier, A., Thompson, L., Yang, D., & Bitz, C. M. (2019). Sustained ocean changes contributed to sudden Antarctic sea ice retreat in late 2016. *Nature Communications*, *10*(1), 14. https://doi.org/10.1038/s41467-018-07865-9

Mollenhauer, G., McManus, J. F., Benthien, A., Müller, P. J., & Eglinton, T. I. (2006). Rapid lateral particle transport in the Argentine Basin: Molecular 14C and 230Thxs evidence. *Deep Sea Research Part I: Oceanographic Research Papers*, *53*(7), 1224–1243. https://doi.org/10.1016/j.dsr.2006.05.005

Müller, J., Massé, G., Stein, R., & Belt, S. T. (2009). Variability of sea-ice conditions in the Fram Strait over the past 30,000 years. *Nature Geoscience*, *2*(11), 772–776. https://doi.org/10.1038/ngeo665

Müller, J., Wagner, A., Fahl, K., Stein, R., Prange, M., & Lohmann, G. (2011). Towards quantitative sea ice reconstructions in the northern North Atlantic: A combined biomarker and numerical modelling approach. *Earth and Planetary Science Letters*, *306*(3), 137–148. https://doi.org/10.1016/j.epsl.2011.04.011

Navarro-Rodriguez, A., Belt, S. T., Knies, J., & Brown, T. A. (2013). Mapping recent sea ice conditions in the Barents Sea using the proxy biomarker IP25: implications for palaeo sea ice reconstructions. *Quaternary Science Reviews*, *79*, 26–39. https://doi.org/10.1016/j.quascirev.2012.11.025

Nihashi, S., & Ohshima, K. I. (2015). Circumpolar Mapping of Antarctic Coastal Polynyas and Landfast Sea Ice: Relationship and Variability. *Journal of Climate*, *28*(9), 3650–3670. https://doi.org/10.1175/JCLI-D-14-00369.1

Ohshima, K. I., Fukamachi, Y., Williams, G. D., Nihashi, S., Roquet, F., Kitade, Y., Tamura, T., Hirano, D., Herraiz-Borreguero, L., Field, I., Hindell, M., Aoki, S., & Wakatsuchi, M. (2013). Antarctic Bottom Water production by intense sea-ice formation in the Cape Darnley polynya. *Nature Geoscience*, *6*(3), 235–240. https://doi.org/10.1038/ngeo1738

Parkinson, C. L. (2019). A 40-y record reveals gradual Antarctic sea ice increases followed by decreases at rates far exceeding the rates seen in the Arctic. *Proceedings of the National Academy of Sciences of the United States of America*, *116*(29), 14414–14423. https://doi.org/10.1073/pnas.1906556116

Prodger, S., Russell, P., Davidson, M., Miles, J., & Scott, T. (2016). Understanding and predicting the temporal variability of sediment grain size characteristics on high-energy beaches. *Marine Geology*, *376*, 109–117. https://doi.org/10.1016/j.margeo.2016.04.003

Rampen, S. W., Abbas, B. A., Schouten, S., & Sinninghe Damste, J. S. (2010). A comprehensive study of sterols in marine diatoms (Bacillariophyta): Implications for their use as tracers for diatom productivity. *Limnology and Oceanography*, *55*(1), 91–105. https://doi.org/10.4319/lo.2010.55.1.0091

Riaux-Gobin, C., Poulin, M., Prodon, R., & Treguer, P. (2003). Land-fast ice microalgal and phytoplanktonic communities (Adélie Land, Antarctica) in relation to environmental factors during ice break-up. *Antarctic Science / Blackwell Scientific Publications*, *15*(3), 353–364. https://doi.org/10.1017/S0954102003001378

Riebesell, U., Schloss, I., & Smetacek, V. (1991). Aggregation of algae released from melting sea ice: implications for seeding and sedimentation. *Polar Biology*, *11*(4), 239–248. https://doi.org/10.1007/BF00238457

Rontani, J.-F., Belt, S. T., Vaultier, F., & Brown, T. A. (2011). Visible light induced photo-oxidation of highly branched isoprenoid (HBI) alkenes: Significant dependence on the number and nature of double bonds. *Organic Geochemistry*, *42*(7), 812–822. https://doi.org/10.1016/j.orggeochem.2011.04.013

Rontani, J.-F., Smik, L., Belt, S. T., Vaultier, F., Armbrecht, L., Leventer, A., & Armand, L. K. (2019). Abiotic degradation of highly branched isoprenoid alkenes and other lipids in the water column off East Antarctica. *Marine Chemistry*, *210*, 34–47. https://doi.org/10.1016/j.marchem.2019.02.004

Saggiomo, M., Poulin, M., Mangoni, O., Lazzara, L., De Stefano, M., Sarno, D., & Zingone, A. (2017). Spring-time dynamics of diatom communities in landfast and underlying platelet ice in Terra Nova Bay, Ross Sea, Antarctica. *Journal of Marine Systems*, *166*, 26–36. https://doi.org/10.1016/j.jmarsys.2016.06.007

Schumacher, B. A. (2002). *Methods for the determination of total organic carbon (TOC) in soils and sediments*. U.S. Environmental Protection Agency, Washington, DC, EPA/600/R-02/069 (NTIS PB2003-100822), 2002.

Scott, P., McMinn, A., & Hosie, G. (1994). Physical parameters influencing diatom community structure in eastern Antarctic sea ice. *Polar Biology*, *14*(8), 507–517. https://doi.org/10.1007/BF00238220

Smik, L. (2016). *Development of biomarker-based proxies for paleo sea-ice reconstructions* (Doctoral dissertation). Retrieved from PEARL. (http://hdl.handle.net/10026.1/8169). Plymouth: University of Plymouth.

Smik, L., Belt, S. T., Lieser, J. L., Armand, L. K., & Leventer, A. (2016). Distributions of highly branched isoprenoid alkenes and other algal lipids in surface waters from East Antarctica: Further insights for biomarker-based paleo sea-ice reconstruction. *Organic Geochemistry*, *95*, 71–80. https://doi.org/10.1016/j.orggeochem.2016.02.011

Spreen, G., Kaleschke, L., & Heygster, G. (2008). Sea ice remote sensing using AMSR-E 89-GHz channels. *Journal of Geophysical Research, C: Oceans*, *113*(C2). https://doi.org/10.1029/2005JC003384

Stein, R., Fahl, K., Schreck, M., Knorr, G., Niessen, F., Forwick, M., Gebhardt, C., Jensen, L., Kaminski, M., Kopf, A., Matthiessen, J., Jokat, W., & Lohmann, G. (2016). Evidence for

ice-free summers in the late Miocene central Arctic Ocean. *Nature Communications*, *7*, 11148. https://doi.org/10.1038/ncomms11148

Stephens, B. B., & Keeling, R. F. (2000). The influence of Antarctic sea ice on glacial–interglacial CO2 variations. *Nature*, *404*(6774), 171–174. https://doi.org/10.1038/35004556

Sun, J., Liu, D., Ning, X., & Liu, C. (2003). Phytoplankton in the Prydz Bay and the adjacent indian sector of the southern ocean during the austral summer 2001/2012 (in Chinese with English abstract). *Oceanologia et Limnologia Sinica*, *34*(5), 519–532. https://doi.org/10.11693/hyhz200305007007

Sun, W., Han, Z., Hu, C., & Pan, J. (2016). Source composition and seasonal variation of particulate trace element fluxes in Prydz Bay, East Antarctica. *Chemosphere*, *147*, 318–327. https://doi.org/10.1016/j.chemosphere.2015.12.105

Taylor, F., McMinn, A., & Franklin, D. (1997). Distribution of diatoms in surface sediments of Prydz Bay, Antarctica. *Marine Micropaleontology*, *32*(3-4), 209–229. https://doi.org/10.1016/S0377-8398(97)00021-2

Thomas, D. N. (2017). *Sea Ice*. John Wiley & Sons.

Van der Jagt, H., Friese, C., & Stuut, J. B. W. (2018). The ballasting effect of Saharan dust deposition on aggregate dynamics and carbon export: Aggregation, settling, and scavenging potential of marine snow. *Limnol. Oceanogr.*, *63*(3), 1386–1394. https://doi.org/10.1002/lno.10779

Vorrath, M.-E., Müller, J., Esper, O., Mollenhauer, G., Haas, C., Schefuß, E., & Fahl, K. (2019). Highly branched isoprenoids for Southern Ocean sea ice reconstructions: a pilot study from the Western Antarctic Peninsula. *Biogeosciences* , *16*(15), 2961–2981. https://doi.org/10.5194/bg-16-2961-2019

Wang, H., Chen, Z., Wang, C., Liu, H., Zhao, R., Tang, Z., & Huang, Y. (2015). Characteristics of grain size in surface sediments from the continental shelf, Prydz Bay, and implications for sedimentary environment (in Chinese with English abstract). *Chinese Journal of Polar research/Jidi Yanjiu*, *27*(4), 421–428. https://doi.org/10.13679/j.jdyj.2015.4.421

Williams, G. D., Herraiz-Borreguero, L., Roquet, F., Tamura, T., Ohshima, K. I., Fukamachi, Y., Fraser, A. D., Gao, L., Chen, H., McMahon, C. R., Harcourt, R., & Hindell, M. (2016). The suppression of Antarctic bottom water formation by melting ice shelves in Prydz Bay. *Nature Communications*, *7*, 12577. https://doi.org/10.1038/ncomms12577

Yoon, H. I., Park, B.-K., Domack, E. W., & Kim, Y. (1998). Distribution and dispersal pattern of suspended particulate matter in Maxwell Bay and its tributary, Marian Cove, in the South Shetland Islands, West Antarctica. *Marine Geology*, *152*(4), 261–275. https://doi.org/10.1016/S0025-3227(98)00098-X

Yu, P., Hu, C., Liu, X., Pan, J., & Zhang, H. (2009). Modern sedimentation rates in Prydz Bay, Antarctic (in Chinese with English abstract). *Acta Sedimentologica Sinica*, *27*(6), 1172–1177.

Zheng, S. (2011). *Effects of sea ice and ice shelf on the ocean processes in Prydz Bay, Antarctica* (in Chinese with English abstract; Doctoral dissertation). Retrieved from CNKI. (https://cnki.net/lunwen-1011231298.html). Qindao: Ocean University of China.

564 **Table 1.** Average of the TOC, Mz, sorting, biomarker data, and satellite-derived austral summer and spring SIC in areas with different
565 sea ice conditions.
566

	TOC (%)	Sorting (φ)	Mean Size (φ)	Brassicasterol (μg/g OC)	HBI III (ng/g OC)	$IPSO_{25}$ (ng/g OC)	P_BIPSO_{25} (c=0.0031)	SIC_{Spr} %	SIC_{Sum} %
Fast ice zone	1.04±0.84	1.88±0.41	4.92±1.63	87.87±32.21	578.58±281.23	791.13±384.58	0.74±0.07	47.48±19.37	47.48±19.37
Non-fast ice zone	0.90±0.40	2.14±0.43	5.37±1.08	98.70±96.63	174.98±194.34	179.49±200.02	0.34±0.18	27.00±12.90	27.00±12.90

567